Tikrit Journal of Engineering Sciences (2025); 32(4): 2217
DOI: http://doi.org/10.25130/tjes.32.4.13

IRAQI Academic Scientific Journals

ISSN: 1813-162X (Print); 2312-7589 (Online)
Tikrit Journal of Engineering Sciences
available online at: http://www.tj-es.com

TJES Tikrit Journal of Engineering Sciences

Shear Capacity- Rotational Relationship of the Normal Reinforced Concrete Beams

Othman M. Abdullah *, *Aziz I. Abdullah*, *Wisam A. Aules*
Department of Civil, Engineering College, Tikrit University, Tikrit, Iraq.

Keywords:
Concrete; Curvature ductility; Mode of failure; Shear force; Shear rotation; Rotation ductility.

Highlights:

- *Three distinct failure modes were observed: shear, combined, and flexural.*
- *Wider stirrup spacing reduced ductility and load resistance significantly.*
- *Curvature increased as shear capacity decreased with high a/d ratios.*
- *Curvature increased as shear capacity decreased.*

ARTICLE INFO
Article history:

Received	06 Jun.	2024
Received in revised form	13 Jul.	2024
Accepted	12 Aug.	2024
Final Proofreading	14 Aug.	2025
Available online	29 Aug.	2025

Citation: Abdullah OM, Abdullah AI, Aules WA. **Shear Capacity- Rotational Relationship of the Normal Reinforced Concrete Beams**. *Tikrit Journal of Engineering Sciences* 2025; **32**(4): 2217.
http://doi.org/10.25130/tjes.32.4.13

*Corresponding author:
Othman M. Abdullah
Department of Civil, Engineering College, Tikrit University, Tikrit, Iraq.

Abstract: This study investigated the shear-rotation relationship of concrete beams under static loading. Nine cantilever beams with section dimensions of (200×300) mm and an effective depth of 266 mm were tested until failure. The study focuses on the effects of varying shear span-to-effective depth ratios (a/d) and spacing between stirrups on the beam's behavior. The (a/d) ratio varied from 2.44 to 4.511, and the shear reinforcement spacing was (75, 100, and 150) mm. The key results included three modes of failure: shear, combined, and flexural failures. The shear failure occurred at an (a/d) ratio of 2.443, combined failure occurred at an a/d ratio of 3 and 3.571, and flexural failure occurred at an a/d ratio of 3.57 and 4.511. The ultimate load capacity of the beams decreased from 11.43% to 35.28% as the a/d ratio increased from 2.443 to 4.51. Curvature ductility increased significantly with high a/d ratios, rising to 174.95% as the (a/d) ratio increased from 2.44 to 3. Also, curvature ductility increased by 183.65% as the (a/d) ratio increased from 2.443 to 4.511. However, it decreased up to 25.98% with larger stirrup spacing, i.e., 150 mm. The shear-rotation demonstrated a significant increase with increasing (a/d) ratio from 2.443 to 3.571, i.e., 92%. However, this increase was accompanied by an increase in the rotation by 81.42% as (a/d) changed from 2.443 to 3.571, and increased to 84.84% as (a/d) changed from 2.443 to 4.511. The shear-plastic rotation relationship indicated that increasing the (a/d) ratio significantly improved ductility and the beam's ability to absorb energy. Increasing the spacing between stirrups adversely affected these properties, leading to reduced ductility, curvature, and load resistance.

العلاقة بين سعة القص والدوران للعتبات الخرسانية الاعتيادية

عثمان مجيد عبدالله، عزيز إبراهيم عبدالله، وسام عامر علص
قسم الهندسة المدنية/ كلية الهندسة / جامعة تكريت / تكريت – العراق.

الخلاصة
بحثت هذه الدراسة علاقة دوران القص للعتبات الخرسانية تحت التحميل الثابت. تم اختبار تسع عتبات ناتئة بأبعاد مقطع (200 ×300) مم، وعمق فعال 266 مم حتى الفشل. وتركز الدراسة تاثير نسب فضاء القص الى العمق الفعال والتباعد بين الركائب على سلوك العتبات. تتراوح نسبة (a/d) من 2.44 إلى 4.511 ، ويتراوح التباعد بين الركائب من 75 مم إلى 150 مم. تستخدم مقاييس الإجهاد ومقاييس تحويل الجهد الخطي المنخفض لقياس الإزاحة والدوران والمطاوعية. وتشمل النتائج الرئيسية ثلاثة أنماط من الفشل: القص، الفشل المركب، وفشل الانحناء : فشل القص يحدث عندما تكون نسبة (a/d) تساوي 2.443 ، الفشل المركب يحدث عندما تكون نسبة (a/d) تساوي 3 ، و 3.571 ، وفشل الانحناء يحدث عندما تكون نسبة (a/d) تساوي 3.57 ، و 4.511. انخفضت قابلية التحمل النهائية للعتبات بنسبة 11.43 ٪ إلى 35.28 ٪ عند زيادة نسبة (a/d) من 2.443 إلى 4.51. زادت مطاوعية الانحناء بشكل ملحوظ مع ارتفاع نسب (a/d)، حيث ارتفعت بنسبة تصل إلى 174.95 ٪ عندما زادت نسبة (a/d) من 2.44 الى 3 وزادت بنسبة 183.65 ٪ عندما زادت نسبة (a/d)من 2.443 إلى 4.511 ولكنها انخفضت بنسبة تصل إلى 25.98 ٪ مع تباعد أكبر للركاب (150) مم) أظهر دوران القص زيادة كبيرة مع زيادة نسب a/d من 2.443 إلى 3.571 ، بزيادة تصل إلى 92٪. وزيادة بنسبة 81.42 ٪ عندما تغير (a/d) من (2.443 إلى 3.571) وزاد إلى 84.84 ٪ عندما تغير (a/d) من (2.443 إلى 4.511). أشارت العلاقة بين الدوران اللدن ومقاومة القص إلى أن زيادة النسب (a/d) حسنت بشكل كبير مطاوعية وقدرة الحزمة على امتصاص الطاقة. أثرت زيادة التباعد بين الركائب سلبا على هذه الخصائص، مما قلل من المطاوعية والانحناء ومقاومة الحمل.

الكلمات الدالة: خرسانة مسلحة، مطاوعية الانحناء، نمط الفشل، قوة القص، دوران القص، مطاوعية الدوران.

1.INTRODUCTION

The relationship between shear capacity and flexural rotation is a critical aspect in the analysis and design of structural components, and it is an important factor in studying and designing elements, especially in structural engineering [1]. This relationship mainly deals with how the cross-sectional materials of the beam behave when subjected to loads. Moreover, shear capacity and flexural rotation have a significant impact on determining various aspects such as the stability, performance of the structural integrity, and the safety of various types of structures, such as buildings, bridges, and other load-bearing elements [2]. Shear capacity refers to the overall ability of a structural component to withstand shear forces without undergoing failure. The shear strength refers to the concrete material's ability to resist shear stresses, which is influenced by factors such as concrete mix and aggregate characteristics. In contrast, shear capacity is the overall ability of a concrete beam to resist shear forces, considering both the concrete's shear strength and the contribution from shear reinforcement. In the concrete, the mechanism of shear stress is affected by several factors, such as the magnitude and distribution of the applied load and the properties of the concrete. In addition, the shear stress can develop cracks or failure planes within the concrete if the applied shear stress exceeds the shear strength of the concrete [3]. In conventional reinforced concrete (RC) beams, shear failure often happens in a plastic state after cracking. Several processes, including aggregate interlock, dowel effect, concrete residual strength throughout the fracture processing zone, and force transmission through the compression chord, resist the shear force during loading [4]. Shear reinforcement, typically embodied by stirrups, improves shear capacity by countering diagonal tension forces. As shear forces increase, diagonal cracking, a clear indicator of approaching shear failure, appears at a 45-degree angle. The shear resistance increased by adding aggregate interlock, which is more evident at increasing coarse aggregate concentration. The shear resistance is greatly influenced by the crucial dimension of effective depth, which is measured from the centroid of the tensile reinforcement to the extreme compression layer. Shear is caused in part by concrete shear friction, which occurs at the interface of tensile and compressed concrete [5]. Flexural rotation in concrete beams is the rotation that occurs in the beam subjected to a bending moment or differential settlement. When external loads are imposed on the element, it undergoes deformation, including translational displacements and angular changes in the structural element's ability to rotate [2]. Studies of statically determinate structures have examined the interplay between rotations and shear forces in critical zones of reinforced concrete members [6]. In a separate experimental study, Vaz Rodriges et al. [7] investigated how shear impacts the rotational capacity of 11 slab strips. It was concluded that decreasing applied shear force values enhanced the rotational capacity of plastic hinges. The most relevant shear design formulas for members with shear reinforcement employed various methods to consider the deformation of critical zones [8]. In reinforced concrete members without shear reinforcement, the rotation capacity decreases as the shear forces increase. This behavior has been experimentally confirmed in shear failures in statically determined beams before and after the flexural reinforcement yielded. The development of shear failures after the yielding of flexural reinforcement occurs because the crack width increases with increasing rotations, leading to a reduction in the shear capacity of the beams. These results show the increased

rotational capacity of the plastic hinges [9]. Shear strength in concrete falls as bending rotation rises in reinforced concrete beams with shear reinforcement because the concrete loses shear strength when the flexural reinforcement yields. This behavior is because the plastic hinge rotation might limit the shear strength capacity [10]. This behavior complies with the Vaz Rodrigues et al. failure criterion [7]. Plastic strains in concrete beams without shear reinforcement are important for assessing rotation capacity at failure. These strains are permanent deformations beyond the elastic limit, mainly in high-stress regions [8]. The ratio of shear span to effective depth of beam, or (a/d) ratio, is the most important factor as far as the behavior of the reinforced concrete beams is concerned. The a/d ratio means that the length of the beam over which shear force is transferred to the concretions [9]. Increasing the a/d ratio decreases the beams' shear capacity; higher ratios mean longer distances for shear force transfer, diminishing the effectiveness of shear reinforcement and concrete. This behavior can lead to a shift from flexural mechanisms to shear failure, characterized by diagonal cracking due to the concrete's inability to resist shear forces effectively. Kim and Park (2007) [10] noted that higher a/d ratios in beams without web reinforcement led to earlier shear failure and reduced shear strength. Design codes like ACI 318 limit the maximum allowable a/d ratio to ensure adequate shear capacity and prevent shear failure. Reza and Maheri (2006) [11] found that an increase in the a/d ratio decreased shear capacity, while beams with lower a/d ratios showed better ductility and serviceability, preventing sudden shear failure. The shear capacity of RC beams decreased with increasing the a/d ratio, mainly due to the long transfer distances, reducing the effectiveness of shear reinforcement and concrete. Larger beams showed greater reductions in shear capacity, while beams with higher a/d ratios increased susceptibility to shear failure, transitioning from ductile flexural to brittle failure modes [12]. Lopes and Do Carmo presented a theoretical model to assess the crucial zone's plastic rotation capability under shear stress [13]. Based on the authors' knowledge, only a few studies have evaluated the shear strength in RC members with a wide range of shear/depth ratios. However, the shear span /depth ratio is an essential component of the shear behavior of RC beams [13]. Some researchers have investigated the effect of the shear span/depth ratio on the shear performances of RC beams, with ratios of shear span/depth ranging from 1.0 to 3.5, to evaluate the strengthening impact for beams showing different shear failure modes. Concrete beams' shear strength increases with the shear span to depth ratio, due to better shear transfer mechanisms over shorter spans. However, as the (a/d) ratio exceeds 2 due to increasing the shear span-to-effective depth ratio, the forces over a greater distance are dispersed. Because the shear forces are less concentrated, the compression zone's effectiveness in transferring shear forces decreases, making it harder for the compressive strut mechanism to function effectively. The beams undergo a transformation from a deep beam to a slender beam. This contribution diminishes. Beyond this, the larger span-to-depth ratio reduces efficiency and decreases strength. Thus, the shear span-to-depth ratio should be well determined when concerned with the behavior of beams [12]. A theoretical model to assess the crucial zone's plastic rotation capability under shear stress was presented by Lopes and Do Carmo [13]. The rotation capacity of the plasticized section depends, namely, on five factors: the concrete compressive strength, cross-section dimension and shape of the beam, the ratio of the shear reinforcement area to the gross area of the section, the element slenderness, and the shear strength [14]. However, the ratio of tensile longitudinal reinforcement, the ductility of reinforcement, and the relationship between bond and slip are the most important and influential elements in the turnover of plastic [14]. The literature review on shear in RC beams reveals a lack of experimental data on the relationship between rotation and shear capacity during loading. This information will help assess structures damaged by shear forces, such as those exposed to earthquakes. The relationship will be crucial in practical and theoretical studies on shear capacity in RC beams. This study investigates the relationship between shear capacity and rotational of concrete beams, focusing on parameters like stirrup spacing and shear span to effective depth ratio. It also investigates the effect of these parameters on failure mode, shear capacity, plastic rotation, and moment-curvature relationship.

2.EXPERIMENTAL PROGRAM

2.1.Materials

In this study, various construction materials, including ordinary Portland cement and river sand, served as the fine aggregate and coarse aggregates with a maximum nominal size of 12.5 mm. The amount of clay and silt in coarse aggregates was less than the limits specified in the Iraqi standard. For steel reinforcement, a 16 mm diameter rebar with a yield stress of 600 MPa was used for longitudinal reinforcement, and a 6 mm diameter bar with a yield stress of 530 MPa was used for stirrups. The physical characteristics of the reinforcing bars were tested according to ASTM A615M standards [15], as outlined in Table 1.

Table 1 The Physical Characteristics of the Reinforcing Bars.

Rebar	Yield stress (fy) (MPa)	Ultimate strength (fu) (MPa)
6 mm	530	549
16 mm	600	650

In this study, the grade C25 concrete used to cast the specimens was designed to have a maximum coarse aggregate size of 12.5 mm and a compressive strength of 25 MPa with a water-cement ratio of 0.45. The specimens were covered with two layers of brown Jute and kept wet for 28 days by wetting twice daily. From the same batch of concrete, three cylinders with dimensions of 150 mm in diameter and 300 mm in height were cast and cured under the same conditions as the beams. The compressive strength of the cylinders was examined on the same day as the beam was tested. Following ASTM C39M-14a [16], the compressive strength of concrete was calculated from the average value of the three cylinders. In addition, the flexural strength of the concrete was obtained, following the American standard specification (ASTM C 78-04) [17]. Three (100×100×500 mm) prisms were tested using a flexural testing machine. Each prism was simply supported and subjected to two concentrated-point loads. Moreover, a standard concrete cylinder. A specimen of (150×300) mm was used to determine the splitting tensile strength (fct), according to (ASTM C496-96) [18]. The specimen was loaded at the center until failure. The digital testing machine was used with a 2000kN capacity.

2.2.Configuration of Specimens

Nine cantilever RC beams were tested under static loading. The support of the cantilever beam corresponds to a rigid column in actual construction, whereas the loading point for the cantilever specimens reflects the zero-moment point. All of the beams have dimensions of 200 mm in width and 300 mm in height, and shear span-to-effective depth ratios (a/d) that range from 2.443 to 4.51. The design of shear reinforcement with spacing of (75, 100, and 150) mm for shear span to-effective depth ratios of 2.44, 3,3.57, and 4.51 was used to determine the mode of failure, i.e., shear, combined, and flexural. The top and bottom were reinforced with flexural reinforcements of (4 ø 16) and (2ø16), respectively. The cross-sectional measurements and reinforcing arrangements of beams are shown in Fig. 1. Table 2 illustrates the details of the four groups of specimens. Three beams in each group had shear span lengths of 650, 800, 950, and 1200 mm. The beams were reinforced on the continuous side with heavy shear reinforcement (ø6mm@50mm) to prevent failure from occurring on the continuous side. The samples were represented by the following symbols: B: Shear reinforcement ratio symbol, S: -Shear Failure Mode, C: - Combined Failure Mode, and F: - Flexural Failure Mode.

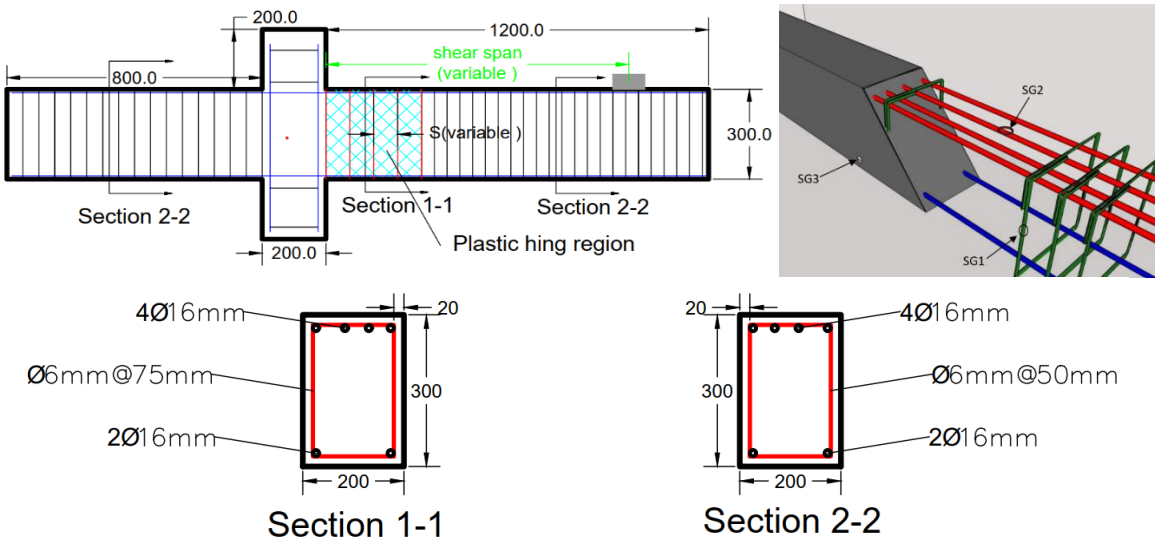

Fig. 1 Beam Details with Strain Gauge Locations.

Table 2 Characteristics of Beams.

#	Beam symbol	Spacing (mm)	Shear reinforcement ratio	Shear span (mm)	(a/d)
1	B1S	75	0.00377	650	2,443
2	B1C	75	0.00377	800	3
3	B1F	75	0.00377	950	3.571
4	B2S	100	0.002827	650s	2.443
5	B2C	100	0.002827	800	3
6	B2F	100	0.002827	950	3.571
7	B3S	150	0.0018846	650	2.443
8	B3C	150	0.0018846	950	3.571
9	B3F	150	0.0018846	1200	4.511

3.3.Loading System and Instrumentation

The test samples were examined at Tikrit University's Structural Testing Laboratory. Figure 2 schematically displays a representative cantilever specimen in the test setup. A 200-ton actuator was utilized to apply a concentrated load vertically at a loading rate of 1 mm/min [19], and 16-channel data loggers were used for data collection. Each beam was equipped with two linear variable displacement transducers (LVDTs), one on top and one on the bottom, to monitor the rotation at the plastic hinge area. Also, a Linear Variable Differential Transformer (LVDT) was used to read the deflection at the end. Electrical strain gauges were installed to monitor the progression of strain in the longitudinal reinforcement, shear reinforcement, and concrete under progressive loading.

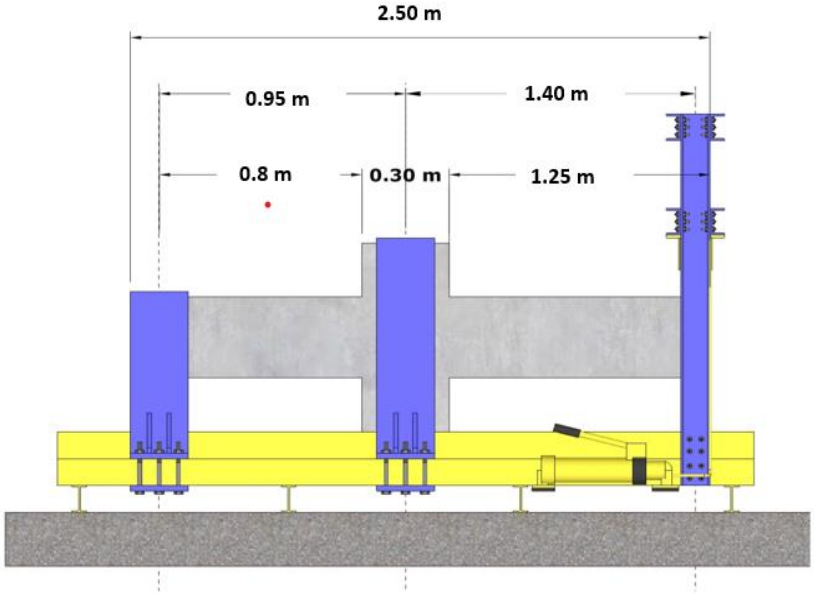

Fig. 2 Diagram of the Beam Test.

3.RESULTS AND DISCUSSION

3.1.Mode of Failure

A reinforced concrete beam may develop many crack patterns throughout the loading process before the beam collapses. The direction and width of these cracks will determine the failure mechanism in concrete structures. In addition, the growth of cracks in concrete is often important to meet standards for serviceability and durability. When shear forces are applied to reinforced concrete beams, shear cracks grow diagonally and incline toward the beam axis [20]. These inclined shear cracks may start inside the web area or as flexural cracks. According to ASCE-ACI Joint Committee 426 (ASCE-ACI 1973) [21], inclined shear fractures can appear either before or after an adjacent flexural crack occurs, and this is what defines the shear failure mechanism in RC beams. Tensile stresses created in the beam, i.e., due to bending moments, lead to flexural cracks. The flexural cracks in reinforced concrete beams usually originate in the tensile area of the concrete. The cracks start in the tension layer of the beam and extend to the compression layer. Different variables, including loading conditions, concrete characteristics, beam geometry, and reinforcement arrangement, might affect the crack pattern [19]. Several factors affect the failure mode, including the shear span to effective depth ratio and stirrup spacing. The mode of failure of specimens with the same condition and with variable values of (a/d) ratio were 2.44, 3,3.57, and 4.51, as given in Fig. 3. For (a/d=2.44), the first crack was flexural cracks occurring in the plastic hinge area, and as the load increased, shear cracks appeared along the plastic hinge region. By the continuous loading process, the shear crack increased, and continuing loading caused shear cracking to progressively progress at a 45-degree angle in the plastic hinge region. With each increase in load, the amount of cracking gradually grew in the same direction and increased in the width of the crack until the beam failed, and the failure type was pure shear failure, as shown in Fig. 3 (a, d, and g). For (a/d= 3), the first crack appeared in the area of the plastic hinge. The crack type was a flexural crack as the load increased, a series of flexural cracks began to appear and increase with increasing load and spread within the plastic hinge area from the top layer of beams and progress toward the bottom layer, and then, at a load progress shear cracks appeared and began to increase concurrently with the flexural cracks until the final failure occurred. The mode of the final failure was a combined failure from the confluence of flexural cracks with shear cracks, as shown in Fig. 3 (b, e, and h). For (a/d= 3.57), as the loading process progressed, some shear cracks appeared and began to

increase with loading. The flexural cracks increased at a higher rate than the shear cracks. With increasing loading, the flexural cracks and their width increased until the final failure occurred, i.e., the type of failure was a flexural failure, as shown in Fig. 3 (c and f). For a large (a/d) value of 4.51, the distance between cracks was considerable, and the width of the cracks was increased. The above results demonstrated that both the rate of crack appearance and the distance between cracks increased as (a/d) increased. This behavior may be explained by the fact that the shorter shear span causes a larger local bond stress along the flexural reinforcement, which results in a bigger moment change per unit length. The results are in agreement with those from a previous study (Hassan *et al.* 1985) [21]. As the a/d ratio increased from 2.44 to 4.571, the ultimate load decreased from 11.43% to 35.28%, as shown in Table 3. The stirrup spacing in each specimen was designed to be 75, 100, and 150 mm. A larger stirrup spacing causes a larger diagonal crack spacing, confirming the idea that the stirrup spacing significantly impacts the distance between shear cracks. As seen from the above analysis and as illustrated by the relation presented in Fig. 4, there was reduction in the load strength of beams when the distance between the stirrups increase, as the cracks appear and spread within the plastic hinge area; however, this behavior is affected by the failure pattern and width of the cracks, whereas stated earlier, increasing the distance between the stirrups increased width of the cracks due to reduction of effective concrete generation of cracks. As the bond effect increased, the transfer length, also known as the crack spacing, reduced. The yield load (Py) of a beam is the load at which the reinforcing steel inside the beam reaches its yield strength. At this point, the steel goes through plastic deformation, which leads to a shift in the beam's behavior from elastic to plastic. The yield load plays a vital role in the design and analysis of reinforced concrete beams. It guarantees the proper functioning of the structure under normal operating conditions and provides adequate warning signs before any potential failure. From the origin point, an inclined straight line is constructed to represent the first line on the load-deflection curve using the junction point of the straight, horizontal line of 0.75P*max*. Then, a horizontal line is drawn from the greatest load P*max* in step two. This method was approved by ACI Committee 374 in 2013. From the intersection point, a vertical line is drawn on the load-deflection curve, and when this line intersects the curve, the point of intersection represents the yield load (Py).

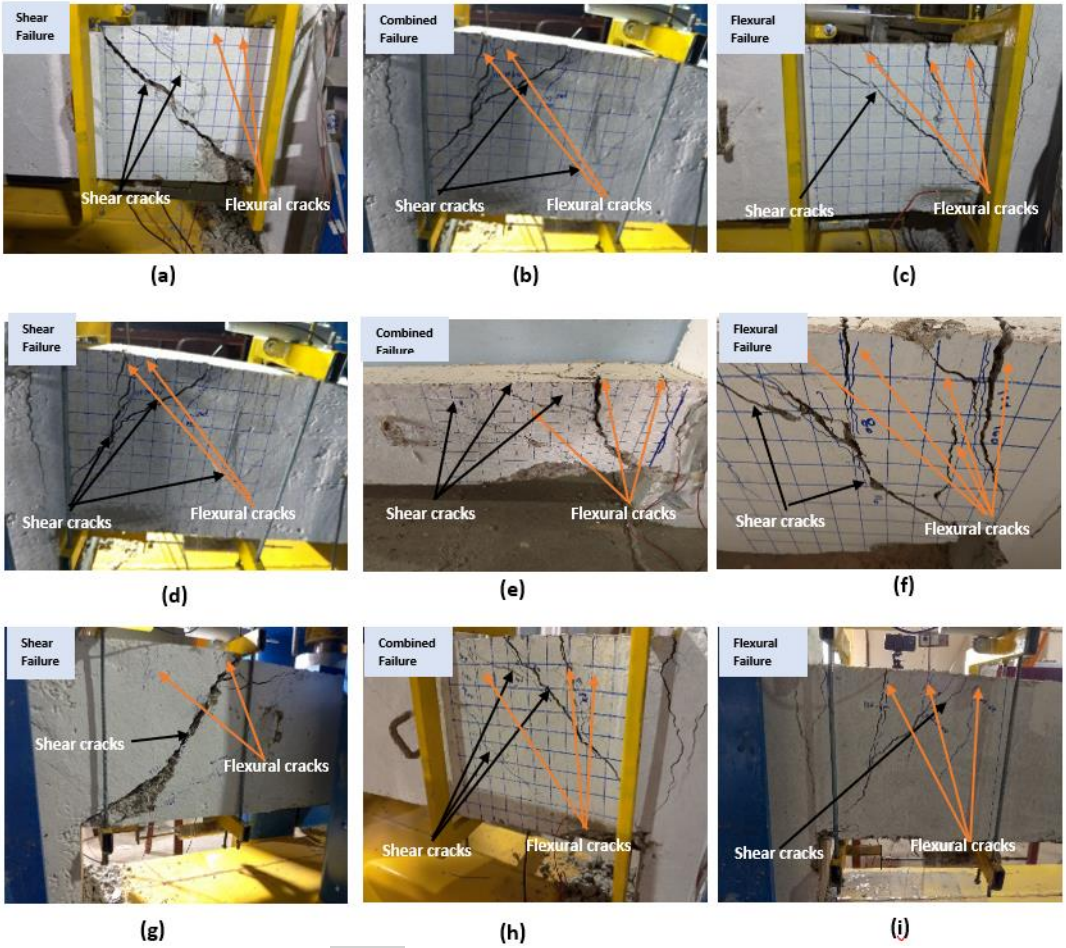

Fig. 3 Modes of Failure for Beams.

Table 3 Ultimate Load and Yield Load Results for Beams.

Symbol	a/d	Shear reinforcement spacing (mm)	Py (KN)	Pu(kN)	Mode Failure
B1S	2.44	75	154.88	189.6	Shear Failure
B2S		100	152.53	186.034	Shear Failure
B3S		150	143.12	174.76	Shear Failure
B1C	3	75	152.8	167.92	Combined Failure
B2C		100	140.67	150.14	Combined Failure
B1F	3.571	75	121.4	128.16	Flexural Failure
B2F		100	107.58	124.97	Flexural Failure
B3C		150	121.23	132.91	Combined Failure
B3F	4.571	150	98.76	113.106	Flexural Failure

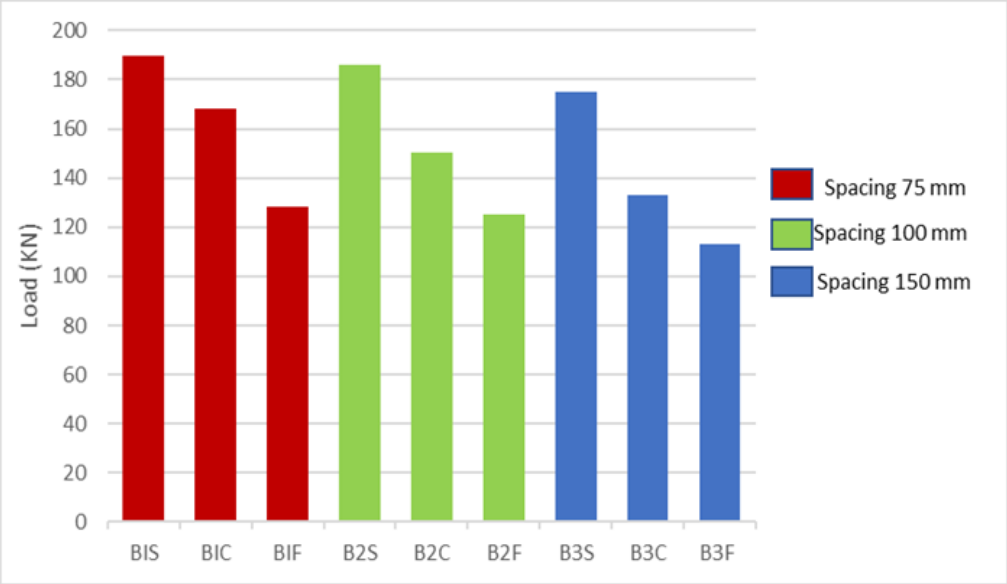

Fig. 4 The Effect of Spacing on Load Capacity.

3.2.Moment - Curvature Relationship and Curvature Ductility

The moment-curvature (M-Φ) relationship defines the flexural behavior of structural elements primarily subjected to bending moments. The ductility of structural elements is also assessed using moment-curvature diagrams, which makes them important in determining how much plastic energy a structural section can absorb [23]. An inelastic curvature denoted as Φp means a curvature assumed by a plastic material of an RC section. When designing a plastic rotation, θp, which is produced by a plastic hinge area, it is vital to consider plastic curvature. When the final curvature is obtained, subtracting the yield curvature provides the plastic curvature needed [23]:

$$\boldsymbol{\Phi p = \Phi u - \Phi y} \qquad \textbf{(1)}$$

where Φu is the ultimate curvature, and Φy *is the yield curvature*. The rotation capacity of the section (θp) is expressed by the product of the average curvature within the plastic hinge domain (κp) and the length of the hinge (LP). The curvature in the direction of the plastic deformation is expected to remain unaltered along the plastic hinge length (LP).

$$\boldsymbol{\theta p = \emptyset p \times Lp} \qquad \textbf{(2)}$$

The Paulay and Priestley (1992) equation was used to compute the plastic hinge length [24], as seen below:

$$\boldsymbol{Lp = 0.08L \times 0.022Fy\ dp} \qquad \textbf{(3)}$$

where L is the shear span length, and db is the diameter of the longitudinal rebar. In an experiment, two LVDTs, one at the top of the beam and another at the bottom of the anticipated plastic hinge region, were used to measure the curvatures at the crucial section along the beam as well as the rotation of the plastic hinge, as seen in Fig. 5.

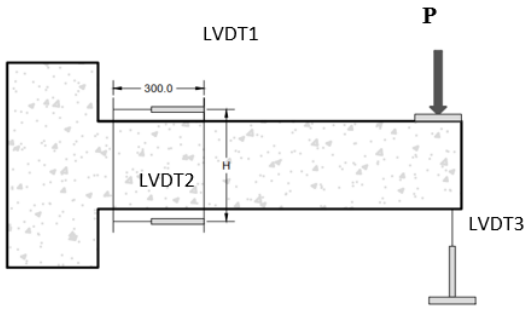

Fig. 5 LVDTs to Measure Beam Curvature.

The ratio of the section's ultimate curvature (Φu) to yield curvature (Φy) is known as curvature ductility. The only variables influencing the structural element's rotation capacity are the length of the plastic hinge, the location of the inelastic curvature, and the curvature applied during the loading action. Curvature ductility significantly affects the overall structural behavior and performance of reinforced concrete beams. The ultimate

flexural capacity of beams with high curvature ductility can be affected by great deflections and deformations that can be experienced before reaching their ultimate strength. Their capacity to support higher loads and provide earlier warning before failure is made possible by this ability. Furthermore, RC beams with high curvature ductility can exhibit ductility, dispersing internal stresses effectively without sudden failure. This behavior is important for allowing safe evacuation and providing warning signals during seismic events or other extreme loading situations. Furthermore, curvature ductility lowers the risk of severe damage by enabling RC beams to absorb energy through plastic deformation during high-loading events like impacts or earthquakes [25]. Curvature ductility helps in controlling the depth and distribution of cracks. Beams with high curvature ductility are more likely to satisfy serviceability and durability criteria and are less likely to fail suddenly. In general, curvature ductility plays a critical role in stress distribution and improves ductile behavior and energy absorption. From Figs. 6, 7, and 8, it was found that increasing the ratio (a/d) led to a significant increase in curvature ductility, where the values for the first group (B1S, B1C, and B1F) increased by 169.9% when the (a/d) ratio was increased from 2.44 to 3 and increased by 115.65% when the (a/d) ratio was increased from 3 to 3.571. While the second group (B2S, B2C, and B2F) increased by 166.85% as the (a/d) ratio increased from 2.44 to 3, and increased by 69.47% as the a/d ratio increased from 3 to 3.571. Moreover, the third group (B3S, B3C, and B3F) increased by 174.95% as the (a/d) ratio increased from 2.44 to 3, and increased by 183.65% as the (a/d) ratio increased from 2.44 to 4.511, as shown in Table 4. The reason for this behavior is that, in reinforced concrete beams, larger shear spans improve predictability and control deformation behavior by producing a more uniform shear stress distribution throughout the beam, leading to high ductility and enabling great deformations before failure. It also increases the proportion of shear force carried by concrete in the compression zone as the shear span increases. On the other hand, short shear spans can frequently be seen in beams with large concentrated loads, which often result in significantly higher shear stresses near the supports, which may cause the formation of diagonal cracks or premature shear failure. This disparate distribution of stress may lead to a sudden brittle failure. Such conditions decrease the beams' ductility, making it more difficult to bend and redistribute loads, particularly when subjected to load. This response is in agreement with Do Carmo *et al.* [26]. By increasing the distance between stirrups by 75, 100, and 150 mm. For (a/d) equals 2.443, increasing the spacing between stirrups from 75mm to 100 mm leads to a decrease in curvature ductility by 4.93 %. In addition, the curvature ductility decreased by 5.8 % for (a/d) was 3. When (a/d) became 3.571, the curvature ductility decreased by 25.98%. Flexural failure causes the most significant decrease in ductility as the distance between stirrups increases. Flexural failure has an active internal distribution of forces, which increases the rate of ductility. Consequently, changing the distance between the stirrups has a greater effect than in the other failure modes, which are less for combined and shear failure, respectively, as previously noted, because the beam curvature decreases if the spacing between stirrups is increased. That increase in the spacing between stirrups leads to an increase in the probability of sudden failure and reduces the ductile behavior by making the beam more susceptible to shear failure, especially in areas with high shear stresses. Furthermore, when the spacing between stirrups is increased, the efficacy of crack control also decreases, as shown in Fig. 3, allowing cracks to distribute and reducing the beam capacity by increasing the width and depth of cracks to undergo significant deformations before failure. Furthermore, shear reinforcement is important to increase energy dissipation with inelastic deformations, including plastic hinge formation and reinforcement yielding. This response is in agreement with Mansour *et. al* [27]. Therefore, it is necessary to maintain sufficient shear reinforcement to ensure the ductile behavior of reinforced concrete beams.

3.3.Yield, Ultimate, and Plastic Curvature

Many definitions of ultimate curvature (Φu) and yield curvature (Φy) have been proposed when the behavior of the RC sections is often not elastic-perfectly plastic under load. A few methods for determining the Φy were proposed by Park (1989). The two most popular methods are shown in Figs. 9 and 10. In Fig. 9, the curve that depicts the meeting point of two lines is referred to as the Φy. From the origin point, an inclined straight line is constructed to represent the first line on the moment-curvature curve using the junction point of the straight, horizontal line of $0.75M\ max$. Draw a horizontal line from the greatest moment $M\ max$ in step two. This method was approved by ACI Committee 374 in 2013. The second method, which equalizes the regions between the line and the envelope of the experimental test above and below the line, is shown in Fig. 10 and aims to meet the equal energy criteria, leading to a modified second-line slope. This approach was accepted in FEMA-440 (2005) [28]. The maximum compressive strength of the concrete is one of the damaged constraints that are used to calculate the longitudinal and transverse

reinforcing steel strain limits. Φm, the ultimate limit of the curvature, was calculated. However, as Fig. 9 illustrates, the method most often used to determine the final curvature was the one corresponding to a 20% reduction in the moment capacity (Saatcioglu and Baingo, 1999) [29]. Inelastic curvature defined by the RC section is referred to as plastic curvature, or Φp. The formation of a plastic hinge region largely depends on the plastic curvature, which defines the plastic rotation θp. The final and yield curvatures are subtracted to determine the quantity of plastic curvature. For the whole plastic hinge length, L, the plastic curvature is thought to be constant.

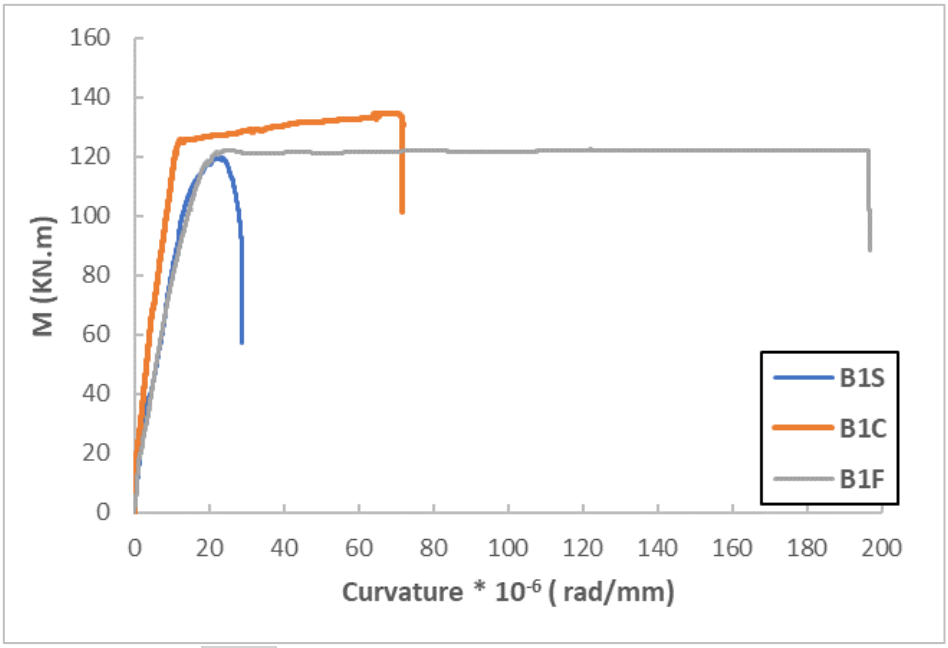

Fig. 6 Moment-Curvature for the First Group.

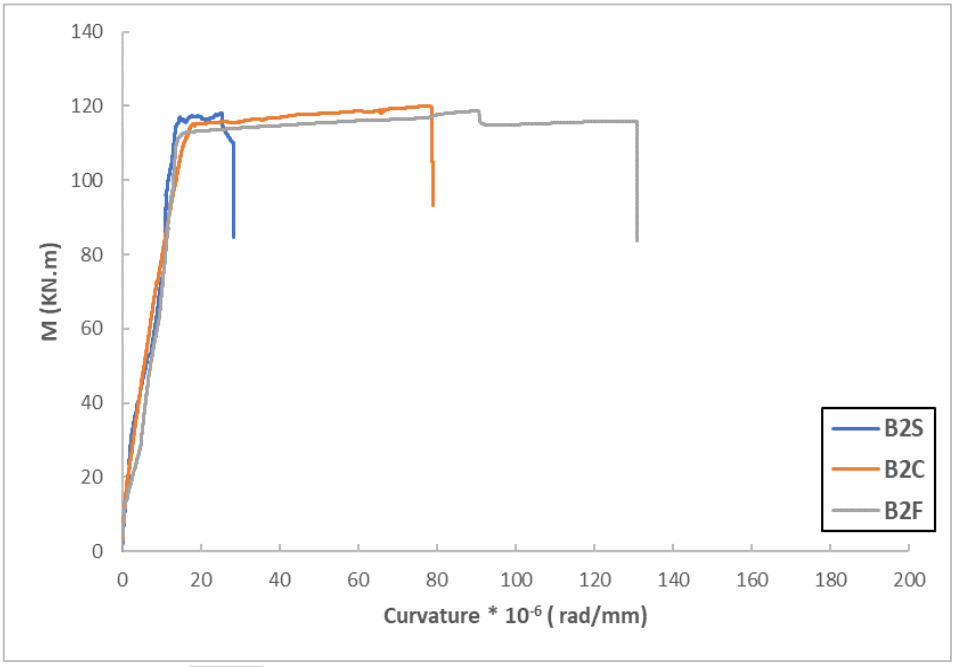

Fig. 7 Moment-Curvature for the Second Group.

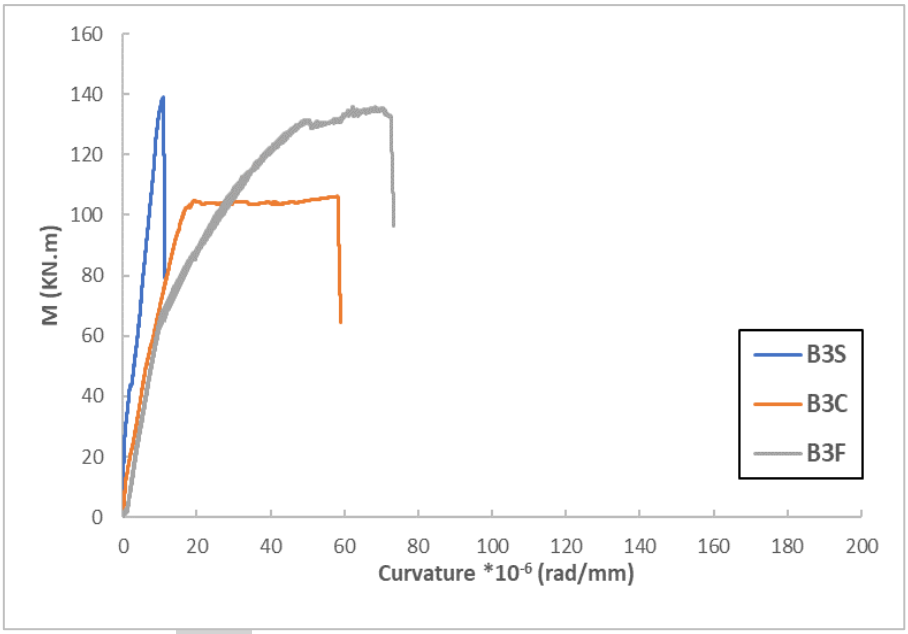

Fig. 8 Moment-Curvature for the Third Group.

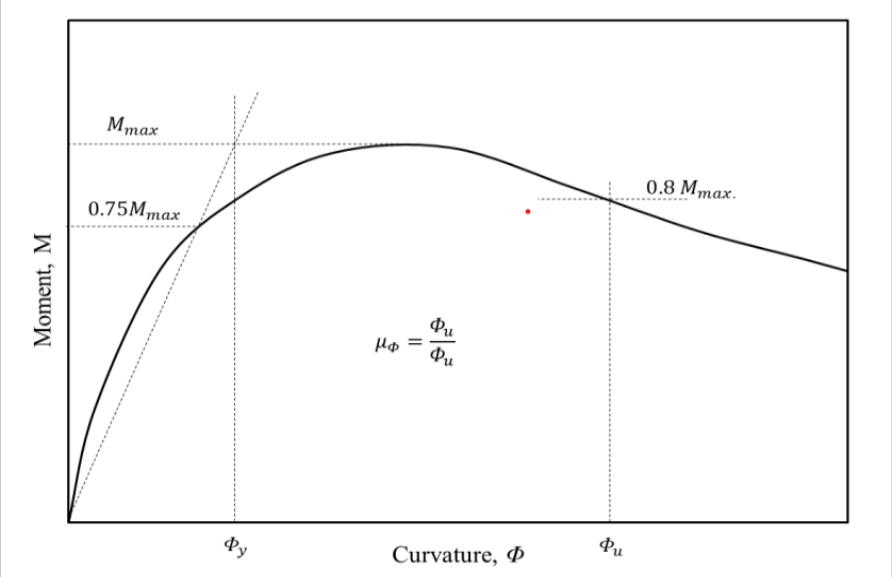

Fig. 9 Definition of Parameters for Curvature (Park [23]).

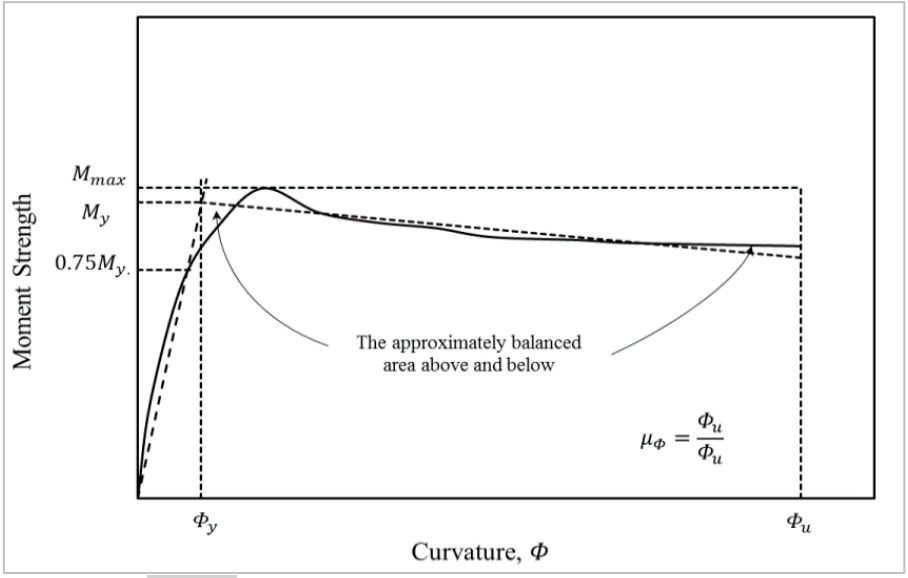

Fig. 10 Definition of Parameters for Curvature [23].

Table 4 The Tested Specimens of Curvature Ductility.

Symbol	Yield Curvature (Φy)	Plastic Curvature (Φp)	Ultimate Curvature (Φu)	Curvature Ductility ($u\Phi$)
B1S	1.50E-05	1.34E-05	2.84E-05	1.8893
B1C	1.4644E-05	5.992E-05	7.4574E-05	5.0922
B1F	1.79E-05	1.79E-04	1.97E-04	10.9818
B2S	1.58E-05	1.26E-05	2.84E-05	1.7961
B2C	1.638E-05	6.198E-05	7.831E-05	4.793
B2F	1.61E-05	1.15E-04	1.31E-04	8.1283
B3S	9.85E-06	1.31E-06	1.12E-05	1.1334
B3C	1.85E-05	3.92E-05	5.77E-05	3.1163
B3F	2.49E-05	5.51E-05	7.99E-05	3.2149

3.4.Shear-Rotation Relationship

Rotation in concrete beams refers to the angular displacement or twist that occurs in a concrete beam when it is subjected to a load. This rotation is an important structural behavior to consider in the analysis and design of concrete beams [30]. The plastic rotation depends on several interrelated factors, which makes the analysis more complicated. Concrete compressive strength, shear span, shear reinforcement ratio, and shear force are some of the basic factors affecting rotation [30, 31]. The relationship between shear capacity and rotation for all beams is given in Fig.11 and illustrated in Table 5. Based on the stirrups spacing and shear span-to-depth ratio, results were divided into three groups, each of which has three beams. For the first group, beams (B1S, B1C, and B1F), the rotation increased 75.6% as (a/d) changed from 2.44 to 3, and 92% as the (a/d) increased to 3.571 with the same stirrup spacing of 75 mm. This behavior is because an increase in shear span indicates a longer shear force acting range, which increases the bending moment and leads to an increase in the rotation of the beam section. In addition, higher shear span-to-depth ratio typically causes the beam to undergo more shear deformation, which might result in increased rotation, and for second group, B2S, B2C, and B2F, with increasing stirrup spacing to 100 mm with the same (a/d) values the rotation increased 60.8% as (a/d) changed from (2.44 to 3), and 86.511% as the (a/d) increased from 2.44 to 3.571. For group three, as the stirrups spacing increased to 150 mm, the rotation increased by 81.42% as (a/d) changed from (2.443 to 3.571) and increased to 84.84% as (a/d) changed from (2.443 to 4.511). Rotation increased as the distance between the stirrups in a reinforced concrete beam decreased. This increase might be because wider spacing reduces beam shear capacity by providing the concrete with less shearing strength, reducing concrete resistance to applied loads, and increasing damage in reinforced concrete sections. Furthermore, the larger spacing makes it difficult to control the width of diagonal tension cracking, resulting in wider cracks and reduced rotation.

3.5.Plastic Rotation

The plastic rotation in concrete beams is an important topic, especially for understanding how reinforced concrete structures behave under loading. A concrete beam will bend elastically under increasing loads until it reaches its yield point. At this point, the steel reinforcement starts to yield. After this, the beam reaches a stage of plastic deformation, in which the deformation continues to increase without the stress increasing along with it [31]. Plastic rotation describes the rotational deformation that occurs at a region where the maximum moment is concentrated in the beam during this plastic deformation, which is important in ensuring structural safety and is measured by the beam's capacity for plastic rotation. The ductility of the beams is defined as the ability to absorb energy and undergo extensive deformation before collapse. The ductile behavior gives structures warning signals and allows loads to be redistributed. The required plastic rotation is not determined by using the section properties alone in analytical and experimental research, which provides the highest possible plastic rotation. Because it depends on several connected parameters, and it is difficult to analyze each one separately, determining the plastic rotation capacity is a difficult challenge. The primary bending parameters for linear elements are the reinforcement ratio, the compressive strength of the concrete, the cross-section's size and shape, the transverse reinforcement ratio, the element's slenderness, and the loading condition. Once the reinforcement yields in the plastic hinge area, the integral of curvatures may be used to compute plastic rotation capacity [31]. Predicting the plastic rotation capacity is easy when the moment curvatures are known. The M–Ø curve characterizes the behavior of the beam section [32]. The results shown in Table 5 and Figs. 12 and 13 indicate that when the distance between the stirrups was constant, the rotation ductility increased by 65.2 % as the (a/d) ratio increased from 2.443 to 3, and 35.8% as (a/d) increased from 3 to 3.571. This behavior might be the mode of failure, gradually changing from shear failure to flexural failure, which is ductile failure. As a result, small shear spans result in sudden shear failures without significant rotation ductility

because the applied shear force is very large close to the support. However, reducing the applied shear on the plastic hinge region increased its deformability. As the spacing between stirrups decreased from 100 mm to 150 mm, the rotation ductility of beams increased by 58.1%. This result means that the beams can undergo larger rotations before failure and generally have a higher shear capacity. Conversely, increasing the spacing between stirrups reduces the beam rotation ductility and shear capacity.

$$\mu = \frac{\theta_u}{\theta_y} \quad (4)$$

Table 5 Rotation of Beams.

Beam	Stirrups Spacing (mm)	(a/d)	Shear Force (kN)	Yield Rotation (rad)	Ultimate Rotation (rad)	Rotation Ductility
B1S	75	2.443	189.6	1.15-03	0.00516	4.481
B1C	75	3	167.925	3.02E-03	0.022372	7.403
B1F	75	3.571	128.16	5.92E-03	0.05952	10.054
B2S	100	2.443	186.034	4.75E-03	0.008531	1.796
B2C	100	3	150.14	4.91E-03	0.023495	4.790
B2F	100	3.571	124.97	1.11E-02	0.063246	5.674
B3S	150	2.443	174.76	2.91E-03	0.003299	1.136
B3C	150	3.571	132.91	5.96E-03	0.01776	2.980
B3F	150	4.511	113.106	5.27E-03	0.02177	4.131

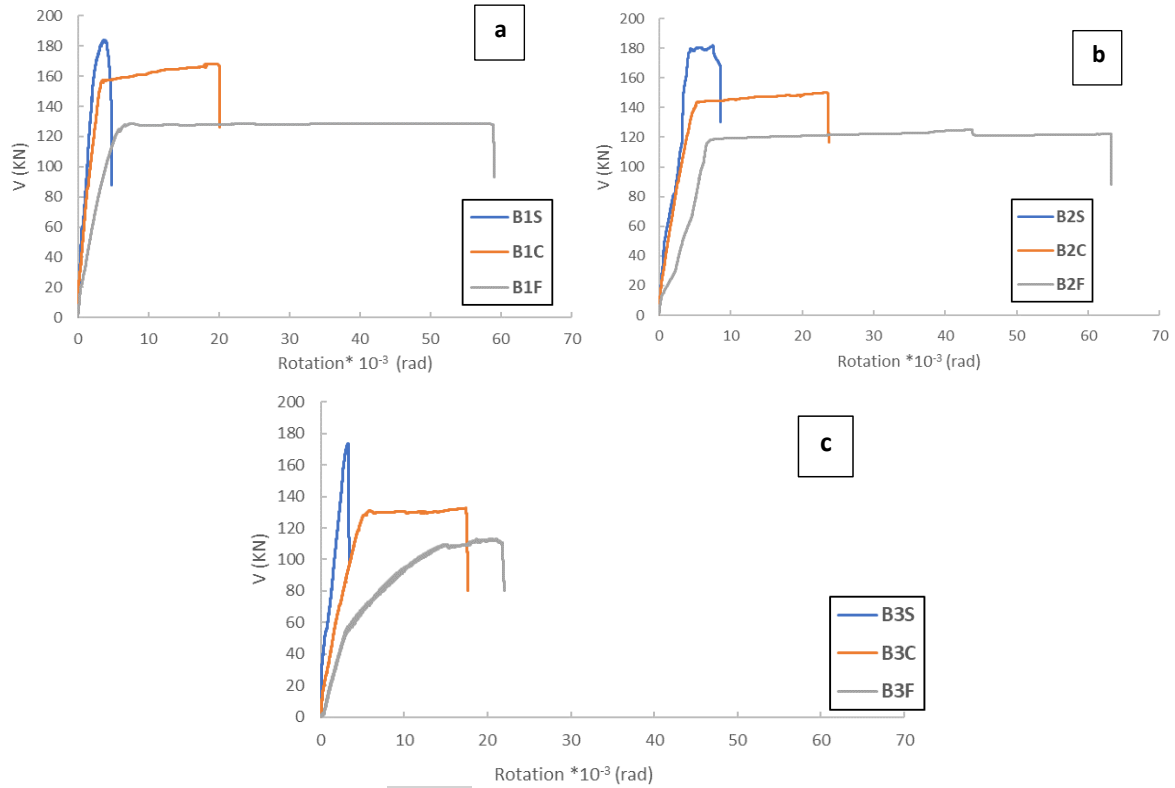

Fig. 11 Shear Force with Rotation.

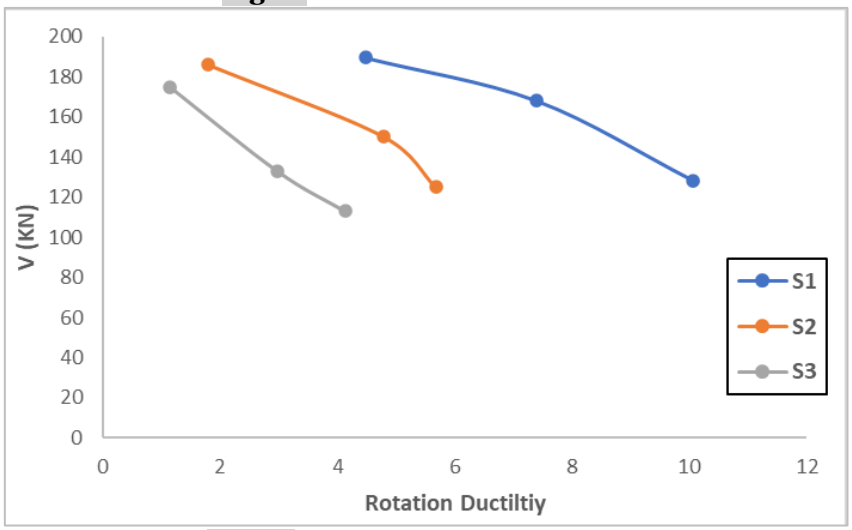

Fig. 12 Rotation Ductility for Beams.

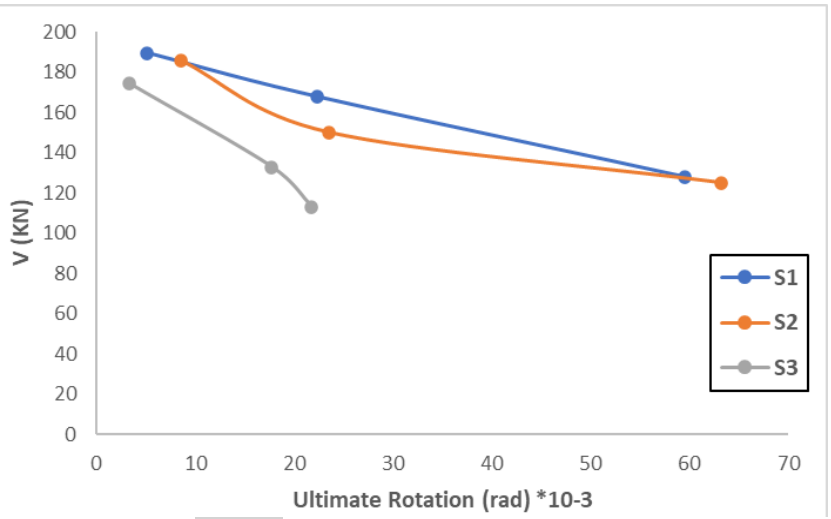

Fig. 13 Ultimate Rotation for Beams.

3.6.Predicting Moment-Curvature

To calculate the moment-curvature curve, the forces in the section must be ascertained step by step with increasing strain. After the tensile and compressive equilibrium was reached, the total moment and curvature were obtained in each step. Since the concrete used in the cover was not reinforced at a strain of 0.003, it must be eliminated from the calculation step. The concrete was crushed. The calculations for the moment and related curvature, as well as the forces related to the concrete and reinforcements in this part, are expressed by Eqs. (5 to 13). The pressures on the concrete and reinforcements in a section with both compressive and tensile rebar are depicted in Fig. 14.

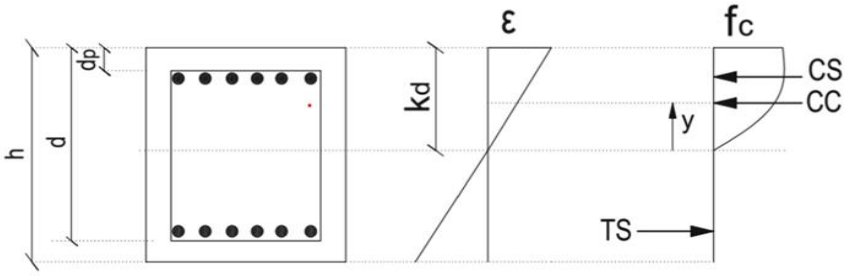

Fig. 14 Concrete and Reinforcement Forces for a Section with Compressive and Tensile Reinforcement.

$$\epsilon_c = \frac{\epsilon ca}{Ci} \times y \quad (5)$$

$$Ac = \int_0^{kd} fc(y)dy \quad (6)$$

$$C = \frac{\int_0^{kd} fc(y) \times y dy}{\int_0^{kd} fc(y)dy} \quad (7)$$

$$CC = Ac \times b \quad (8)$$

$$TS = As \times E \times \epsilon_s \quad (9)$$

$$CS = As^{\sim} \times E \times \epsilon_s^{\sim} \quad (10)$$

$$R = CC + CS - TS \quad (11)$$

$$M = CC \times (d - Ci + C) + CS \times (d - dp) \quad (12)$$

$$\Phi = \frac{\epsilon ca}{Ci} \quad (13)$$

where ∈ca = Concrete Strain that is assumed, Ci = Depth of Natural Axis that must be assumed, b = width of section, Ac = Stress Area of Concrete, C = Centroid of concrete force, CC = Concrete force, CS = Compressive rebars force, TS = Tensile rebars force, R = Equilibrium of forces (must be zero), M = Moment, and φ = Curvature. The procedure for computing the moment-curvature method is displayed in Fig. 15. First, input data are supplied, including the area of reinforcement, section dimensions, and compressive strength of unconfined concrete. Then, using models like Kent Park and Mander, computations are conducted to determine parameters like fc (compressive strength of confined concrete) and the ultimate strain of the confined concrete [33]. After that, the cross-section's force equilibrium is examined to make sure that compressive and tensile forces are balanced. If equilibrium is reached, the values of the moment and curvature are calculated. The compressive strain is progressively increased during this repeated procedure until the portion collapses. Furthermore, when the concrete fracture strain is attained, the section's unconfined concrete cap is progressively removed. The algorithm goes into depth about these processes. The analysis requires the removal of the concrete cover due to its lack of confinement, as shown in Fig. 16 of the algorithm. Concrete cover removal occurred when the strain in the concrete compressive fiber approached approximately 0.003.

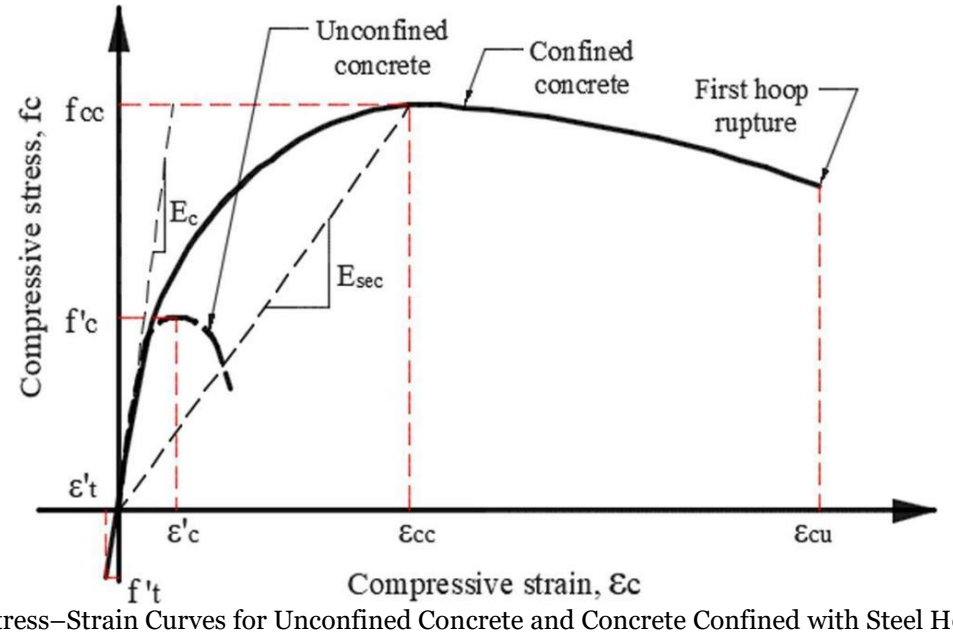

Fig. 15 Stress–Strain Curves for Unconfined Concrete and Concrete Confined with Steel Hoops [32].

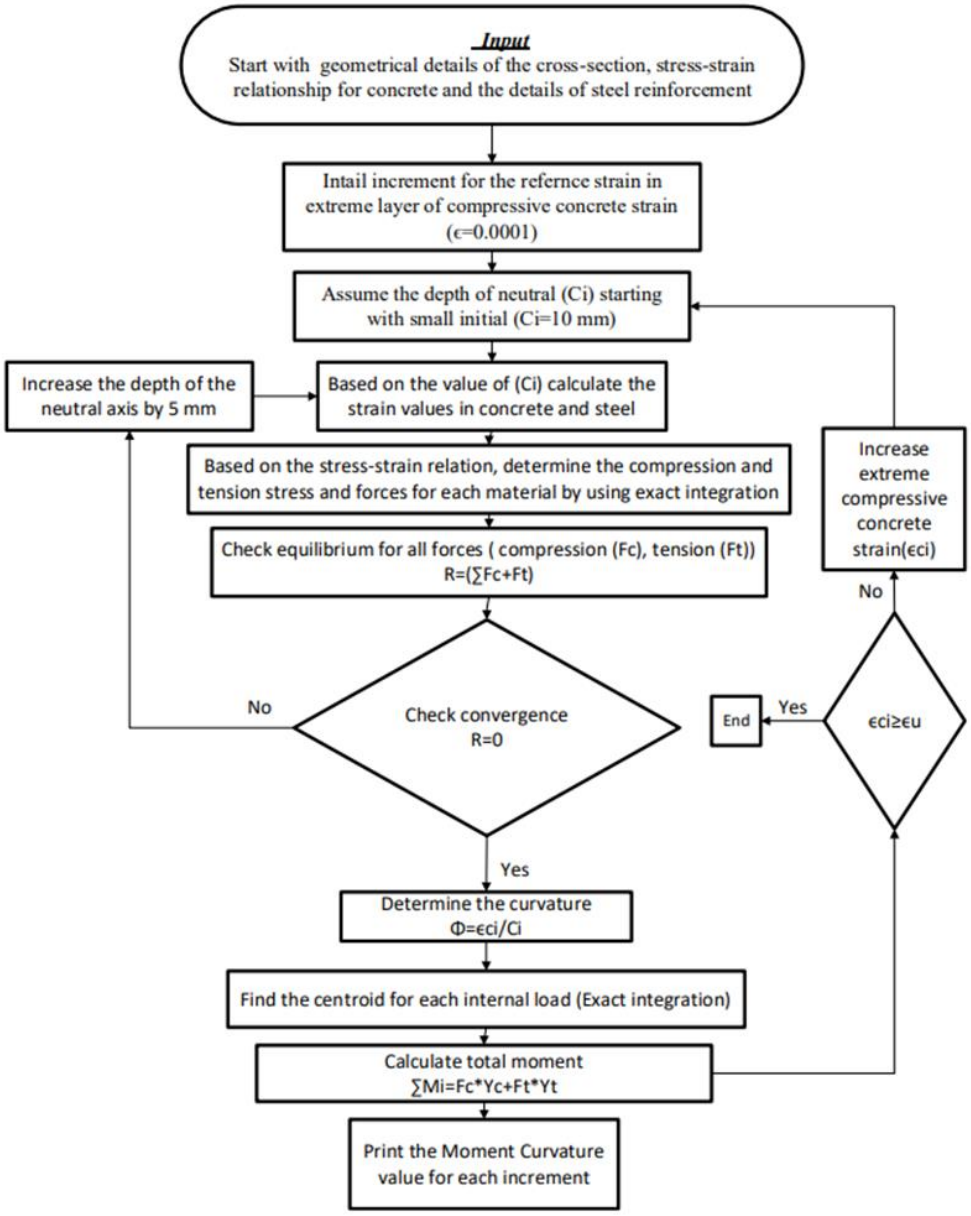

Fig. 16 Proposed Alogrithm for Moment-Curvature Calculation.

For the rectangular reinforced concrete sections used in this experiment, the moment-curvature diagram is displayed in Fig. 17. It should be noticed that the unconfined concrete's compressive strength (Fc = 25 N/mm² assumed) and the reinforcement yielding strength (*Fy* = 600 N/mm²) are related. In this part, MATLAB software is used to compare the Moment-Curvature results from experimental work. The Graphs in Figs. 18, 19, and 20 suggest this formula. In these Figures, the moment-curvature diagrams for the three sections are displayed. Initially, the moment is directly correlated with curvature; the greater the curvature, the greater the moment. When the moment-curvature curve reaches another peak and maximum moment, it then flattens out after a certain stage in the tensile zone. This behavior reduces the strength and bending moment proportionately and causes the concrete's compressive layer to be gradually subjected to increased curvature and strain. As a result, the concrete's exposed surface eventually breaks. The concrete experiences an increase in curvature until it reaches its maximum strain, at which time the cross-section can no longer undergo any further deformation. Comparing the experimental and theoretical values displays that the algorithm developed in this research, for evaluating the moment-curvature diagram in confined reinforced concrete areas, is consistent with the experimental outcomes. If the kind of failure is pure shear, a considerable difference between the practical and theoretical sides is observed. The outcome, depicted in Fig. 21 and Table 5, show that increasing the distance between stirrups significantly increased the difference between experimental and theoretical results. For the first group, the experimental and theoretical results showed a slight difference of 1.06% in sample B1S. However, as the ratio (a/d) increased for the same group, the difference between the results significantly increased. As the distance between stirrups increased from 75 to 100 mm, the percentage of difference increased to 3.92% for the same value of (a/d), i.e., 2.44, and to 39.37% when the distance increased to 150 mm. In conclusion, the value of curvature ductility decreased, and the value of the differences between the experimental and theoretical results increased with increasing stirrup distance and (a/d) ratio.

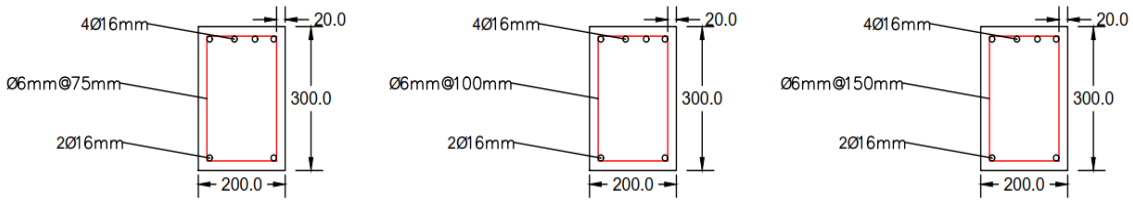

Fig. 17 Reinforced Concrete Sections Used in the Present Study for All Beams.

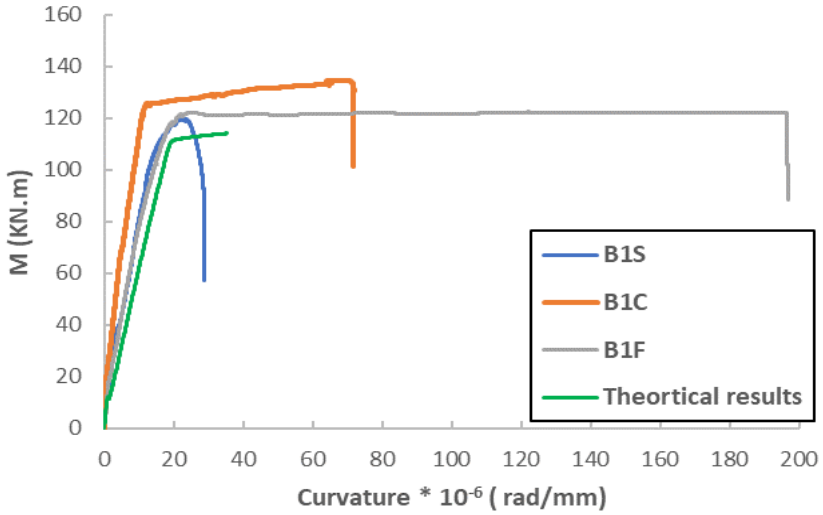

Fig. 18 Comparison of Moment-Curvature Diagrams for the First Group.

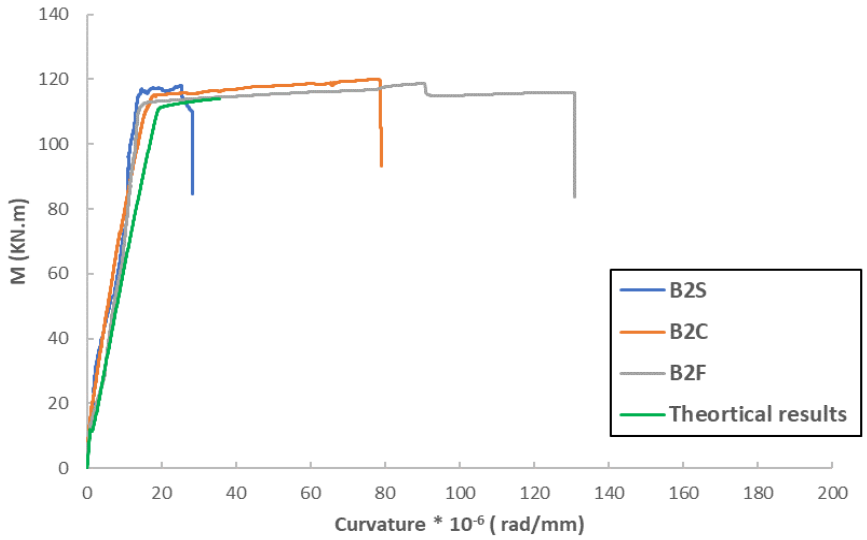

Fig. 19 Comparison of Moment-Curvature Diagrams for the Second Group.

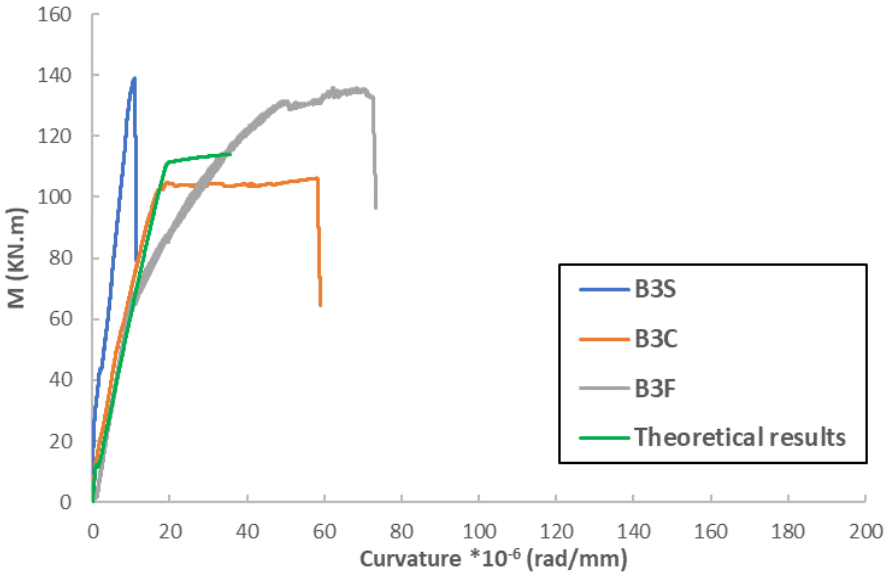

Fig. 20 Comparison of Moment-Curvature Diagrams for the third group.

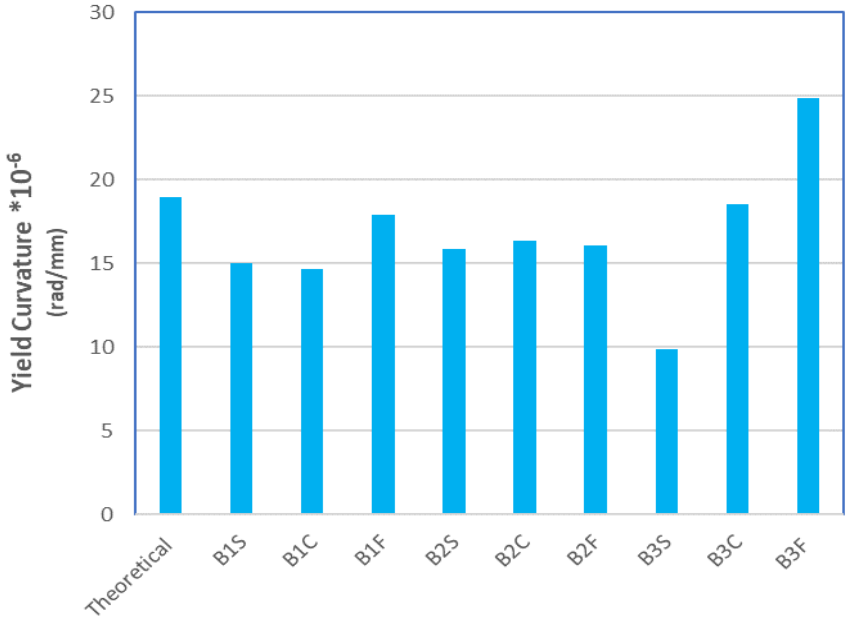

Fig. 21 Comparison of Yield, Ultimate, and Curvature Ductility for Beams.

4.CONCLUSIONS

The conclusions drawn from the present study are as follows:

- The study reveals that higher shear span-to-effective depth ratios (a/d) in concrete beams increase their ductility due to increased deformability and distributed cracking, and increase the beam's flexural deformability.
- Higher shear span-to-effective depth ratios enhance moment and deformability before failure by increasing the beam's flexural deformability. The increased rotation observed with higher ratios is due to improved deformability, allowing for greater internal stress redistribution and increased rotation capacity.
- Increasing the shear span-to-effective depth ratio leads to an increase in the absorption of energy and results in larger deformations under loading.
- The increase in the spacing between stirrups decreases the rotational ductility, making the beams more susceptible to sudden failure.
- Reducing the spacing between stirrups enhances the ultimate rotation value and rotation ductility of the beams.
- Comparison of experimental and theoretical results showed a good agreement, especially when the failure mechanism is pure shear.

ACKNOWLEDGEMENTS

The authors are grateful for the support towards this research by the Civil Engineering Department, College of Engineering, Tikrit University. Postgraduate Research. According to the University Decree No. (3/7/11211) in 28/10/2020.

REFERENCES

[1] Shu Z, Li Z, Yu X, Zhang J, He M. **Rotational Performance of Glulam Bolted Joints: Experimental Investigation and Analytical Approach**. *Construction and Building Materials* 2019; **213**: 675–695.

[2] Cladera A, Marí AR. **Shear Design Procedure for Reinforced Normal and High-Strength Concrete Beams Using Artificial Neural Networks. Part I: Beams Without Stirrups**. *Engineering Structures* 2004; **26**(7): 917–926.

[3] Case J, Chilver AH. **Strength of Materials: An Introduction to the Analysis of Stress and Strain**. Elsevier; 2013.

[4] Zhao DB, Yi WJ, Kunnath SK. **Shear Mechanisms in Reinforced Concrete Beams Under Impact Loading**. *Journal of Structural Engineering* 2017; **143**(9): 04017089.

[5] Gomes TA, de Resende TL, Cardoso DCT. **Shear-Transfer Mechanisms in Reinforced Concrete Beams with GFRP Bars and Basalt Fibers**. *Engineering Structures* 2023; **289**: 116299.

[6] Lopes SM, do Carmo RN. **Deformable Strut and Tie Model for the Calculation of the Plastic Rotation Capacity**. *Computers & Structures* 2006; **84**(31-32): 2174–2183.

[7] Vaz Rodrigues R, Muttoni A, Fernández Ruiz M. **Influence of Shear on Rotation Capacity of Reinforced Concrete Members Without Shear Reinforcement**. *ACI Structural Journal* 2010; **107**(5): 516–525.

[8] Muttoni A, Fernández Ruiz M. **Shear Strength of Members Without Transverse Reinforcement as Function of Critical Shear Crack Width**. *ACI Structural Journal* 2008; **105**(2): 163–172.

[9] López AM, Sosa PFM, Senach JLB, Prada MÁF. **Influence of the Plastic Hinge Rotations on Shear Strength in Continuous Reinforced Concrete Beams with Shear Reinforcement**. *Engineering Structures* 2020; **207**: 110242.

[10] Li W, Leung CK. **Effect of Shear Span-Depth Ratio on Mechanical Performance of RC Beams Strengthened in Shear with U-Wrapping FRP Strips**. *Composite Structures* 2017; **177**: 141–157.

[11] Lubell AS, Bentz EC, Collins MP. **Influence of Longitudinal Reinforcement on One-Way Shear in Slabs and Wide Beams**. *Journal of Structural Engineering* 2009; **135**(1): 78–87.

[12] Somboonsong W, Ko FK, Harris HG. **Ductile Hybrid Fiber Reinforced Plastic Reinforcing Bar for Concrete Structures: Design Methodology**. *ACI Materials Journal* 1998; **95**(6): 655–666.

[13] Do Carmo RNF, Lopes SM. **Influence of the Shear Force and Transverse Reinforcement Ratio on Plastic Rotation Capacity**. *Structural Concrete* 2005; **6**(3): 107–117.

[14] Olalusi OB. **Reliability Assessment of Shear Design Provisions for Reinforced Concrete Beams with Stirrups**. Doctoral Dissertation, Stellenbosch University, Stellenbosch; 2018.

[15] ASTM A. **A615 Standard Specification for Deformed and Plain Carbon-Steel Bars for Concrete**

Reinforcement. ASTM International, West Conshohocken, PA; 2016.

[16] ASTM International. **ASTM C39M-14a: Standard Test Method for Compressive Strength of Cylindrical Concrete Specimens**. ASTM International; 2014.

[17] ASTM C. **Standard Test Method for Flexural Strength of Concrete**. ASTM International, West Conshohocken, PA; 2004.

[18] ASTM C496/C496M-02. **Standard Test Method of Splitting Tensile Strength of Cylindrical Concrete Specimens**. ASTM International; 2002.

[19] Carpinteri A, Carmona JR, Ventura G. **Failure Mode Transitions in Reinforced Concrete Beams--Part 2: Experimental Tests**. *ACI Structural Journal* 2001; **108**(3): 154–162.

[20] Zakaria M, Ueda T, Wu Z, Meng L. **Experimental Investigation on Shear Cracking Behavior in Reinforced Concrete Beams with Shear Reinforcement**. *Journal of Advanced Concrete Technology* 2009; **7**(1): 79–96.

[21] ACI-ASCE Committee 426. **Shear Strength of Reinforced Concrete Members**. *ASCE Proceedings* 1973; **99**(ST6): 1091–1188.

[22] Hassan HM, Ueda T, Tamai S, Okamura H. **Fatigue Test of Reinforced Concrete Beams with Various Types of Shear Reinforcement**. *Transaction of JCI* 1985; **7**: 277–284.

[23] Park R. **Ductility Evaluation from Laboratory and Analytical Testing**. *Proceedings of the 9th World Conference on Earthquake Engineering*; 1988; Tokyo-Kyoto, Japan; **8**: 605–616.

[24] Paulay T, Priestley MN. **Seismic Design of Reinforced Concrete and Masonry Buildings**. John Wiley & Sons, New York; 1992.

[25] Foroughi S, Yuksel SB. **A New Approach for Determining the Curvature Ductility of Reinforced Concrete Beams**. *Slovak Journal of Civil Engineering* 2022; **30**(1): 8–20.

[26] Do Carmo RN, Lopes SM. **Ductility and Linear Analysis with Moment Redistribution in Reinforced High-Strength Concrete Beams**. *Canadian Journal of Civil Engineering* 2005; **32**(1): 194–203.

[27] Mansor AA, Mohammed AS, Salman WD. **Effect of Longitudinal Steel Reinforcement Ratio on Deflection and Ductility in Reinforced Concrete Beams**. *IOP Conference Series: Materials Science and Engineering* 2020; **888**(1): 012008.

[28] FEMA. **Improvement of Nonlinear Static Seismic Analysis Procedures**. FEMA-440, Redwood City; 2005.

[29] Saatcioglu M, Baingo D. **Circular High-Strength Concrete Columns Under Simulated Seismic Loading**. *Journal of Structural Engineering* 1999; **125**(3): 272–280.

[30] Al-Salim NH, Jaber MH, Hassan RF, Mohammed NS, Hussein HH. **Experimental Investigation of Compound Effect of Flexural and Torsion on Fiber-Reinforced Concrete Beams**. *Buildings* 2023; **13**(5): 1347.

[31] López AM, Sosa PFM, Senach JLB, Prada MÁF. **Influence of the Plastic Hinge Rotations on Shear Strength in Continuous Reinforced Concrete Beams with Shear Reinforcement**. *Engineering Structures* 2020; **207**: 110242.

[32] Gusella F. **Effect of the Plastic Rotation Randomness on the Moment Redistribution in Reinforced Concrete Structures**. *Engineering Structures* 2022; **252**: 113652.

[33] Mander JB, Priestley MJ, Park R. **Theoretical Stress-Strain Model for Confined Concrete**. *Journal of Structural Engineering* 1988; **114**(8): 1804–1826.